Real-Time Multiterminal Fault Location System for Transmission Networks

Yanfeng Gong, Mangapathirao Mynam, Armando Guzmán, and Gabriel Benmouyal,
Schweitzer Engineering Laboratories, Inc.
Boris Shulim, *Orange and Rockland Utilities, Inc.*

***Abstract*—Fault location information is critical for operating and maintaining transmission networks. Some of the challenges in calculating accurate fault location include fault resistance, zero-sequence mutual coupling, load, system nonhomogeneity, and transmission lines composed of multiple sections with considerably different characteristics. This paper presents a fully automated real-time fault location system that provides accurate fault location information for multiple transmission lines and makes the results available to system operators and maintenance personnel. The system is capable of the following:**

- **Retrieves all triggered event reports from relays and digital fault recorders (DFRs) automatically. With these reports, the system identifies the faulted transmission line(s) within the transmission network.**
- **Determines the fault type and calculates the fault location and fault resistance using multiterminal fault location methods for different types of power lines, including overhead lines, underground cables, and composite lines that include both overhead line and underground cable sections.**
- **Uses fault location methods that are accurate under fault resistance, parallel-line mutual coupling, system nonhomogeneity, and load.**
- **Supports event reports with a fixed sampling rate or a variable sampling rate that is a multiple of the power system operating frequency.**
- **Supports event reports generated by relays and DFRs connected to an IRIG-B time source.**

This paper compares fault location results calculated from field event reports and reports that are obtained from models of real power systems with actual fault locations.

I. Introduction

Fault location in protective relays has been available for over 20 years. These relays use impedance-based fault location algorithms, typically from one terminal of the transmission line [1] [2]. While these relays have been very useful in locating the majority of faults, the following conditions can affect their fault location accuracy:

- High-resistance faults
- Heavy load conditions
- Zero-sequence mutual coupling

Two-end fault location methods minimize these errors. Reference [3] describes a two-end method based on negative-sequence quantities that can be implemented within line protection relays using the relay programming abilities. Reference [4] describes an implementation of this algorithm using two line relays with relay-to-relay communication to calculate the fault location in real time.

Variable fault resistance introduces errors in fault location estimation; accurate time stamping of the measurements aids in minimizing these errors when using two-end methods.

Synchrophasor technology is promising; however, available message rates make using this technology challenging, especially in applications with fast fault-clearing times.

Alternative traveling wave fault location technology is available and provides good results, but deployment has been limited to extra-high-voltage applications because of its high cost. One of the objectives of the system proposed in this paper is to provide an economical solution using relays that perform line protection functions.

While present two-end fault location methods provide good results in applications where the X/R ratio of the line is constant, they are not suitable for lines with multiple sections. These sections have different impedance characteristics, especially for applications that combine overhead lines and underground cables. This paper presents a method that is based on the negative-sequence voltage profile along the line and is suitable for composite lines.

We use field and laboratory cases where the fault location is known to determine the accuracy of the proposed method. The field case shows that the fault location estimation is off by 475 feet in a 26.3-mile composite line application.

We introduce a real-time fault location system that uses line protection relays and displays fault location information at the control center within 1 minute after the fault occurrence when using Ethernet-based communication. The fault location system automatically retrieves event reports from relays after a fault occurs. The system accommodates event reports with both fixed and variable sampling rates.

Orange and Rockland Utilities, Inc. (ORU) plans to deploy this system in its transmission network and communicate the fault location results to the ORU Energy Control Center.

II. Existing Multiterminal Fault Location Methods

Two-end-based algorithms offer significant advantages in fault location accuracy compared with single-end fault location algorithms. These algorithms are not affected by fault resistance, load, and zero-sequence mutual coupling. Fig. 1 shows the circuit model of a two-bus system with a fault at *m* distance from Terminal X.

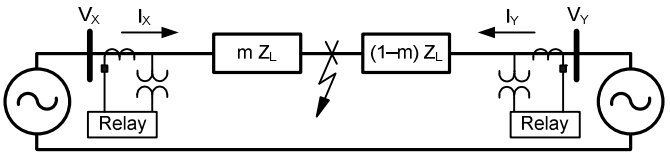

Fig. 1. Circuit model of a two-bus system with a fault at *m* distance from Terminal X.

Some two-end impedance-based fault location algorithms use voltage and current measurements from both terminals of the transmission line to estimate the distance to the fault, *m*, in per unit, according to (1).

$$m = \frac{V_X - V_Y + I_Y \bullet Z_L}{\left(I_X + I_Y\right) \bullet Z_L} \quad (1)$$

V_X and I_X correspond to the voltage and current phasors at Terminal X. V_Y and I_Y correspond to the phasors at Terminal Y. These phasors can be obtained from symmetrical or Clarke components or phase quantities. Z_L is the line impedance. We can compensate Z_L in (1) according to the distributed parameter line model to accommodate long transmission lines [1].

Alignment of local and remote measurements is critical for obtaining accurate fault location using two-end-based algorithms for faults with variable resistance. Methods based on (1) are sensitive to the errors in measurement alignment.

Reference [3] describes a two-end method that uses only negative-sequence quantities and solves a second-order polynomial equation to estimate the distance to the fault. These quantities include local current and voltage measurements, as well as remote source impedance and current magnitudes. Reference [5] presents a method that uses an iterative process to estimate a factor that compensates the error in alignment and then solves the distance to the fault.

Reference [6] uses time-synchronized phasor measurements for multiterminal-based fault location. However, most phasor measurement units (PMUs) offer a maximum data transfer rate of 60 messages per second. Fast clearing times reduce the available fault data, making the synchrophasor-based fault location calculation challenging.

We can use two-end methods to calculate fault location on three-terminal lines by reducing the three-terminal network to a two-terminal network [3]. Fig. 2 shows a typical three-terminal line. For a fault on Section X, the voltages at the tap (V_{TAP}) calculated from Terminal Y and Terminal Z are equal, and the voltage calculated from Terminal X is different from the voltages calculated from the other two terminals. Based on this concept, Section X can be identified.

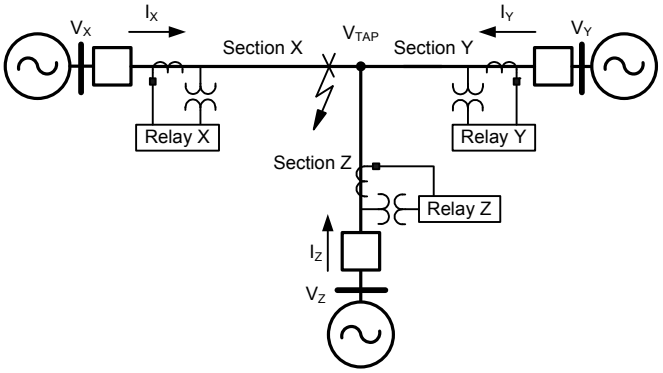

Fig. 2. Three-terminal line with a fault on Section X.

The two-end impedance-based fault location algorithms discussed above assume that power lines are homogeneous with a constant X/R ratio. This assumption introduces errors for nonhomogeneous lines with overhead sections having different line impedances or a combination of underground cable and overhead line sections. This paper describes a new fault location method for homogeneous and nonhomogeneous lines.

III. Considerations for Variable Fault Resistance

Variable fault resistance affects the voltages and currents that the relays at each terminal measure. Fig. 3 shows the sum of the local and remote residual currents (total residual current) and the estimated fault resistance for a B-phase-to-ground fault. The total residual current is approximately equal to the total fault current at the fault location. The fault occurred on a 400 kV transmission line with a line length of 225 kilometers; wildfires close to the transmission line caused the fault condition. Observe that the fault current starts with a peak value lower than 828 A that increases to a peak value of 3,860 A in 4 cycles at a rate of 758 A per cycle. The corresponding resistance that we calculate according to (2) changes at the beginning of the fault and settles to approximately 3 Ω after 4 cycles [1].

$$R_F = \text{real}\left\{\frac{V_{XB} I_{YBk0} + V_{YB} I_{XBk0} - Z_{L1} I_{YBk0} I_{XBk0}}{\left(I_{XBk0} + I_{YBk0}\right)^2}\right\} \quad (2)$$

where:

$$I_{XBk0} = I_{XB} + k_0 I_{XR}$$

$$I_{YBk0} = I_{YB} + k_0 I_{YR}$$

$$k_0 = \frac{Z_{L0} - Z_{L1}}{3Z_{L1}}$$

V_{XB} is the B-phase voltage at Terminal X.
V_{YB} is the B-phase voltage at Terminal Y.
I_{XB} is the B-phase current at Terminal X.
I_{YB} is the B-phase current at Terminal Y.
I_{XR} is the residual current at Terminal X.
I_{YR} is the residual current at Terminal Y.
Z_{L1} is the positive-sequence line impedance.
Z_{L0} is the zero-sequence line impedance.

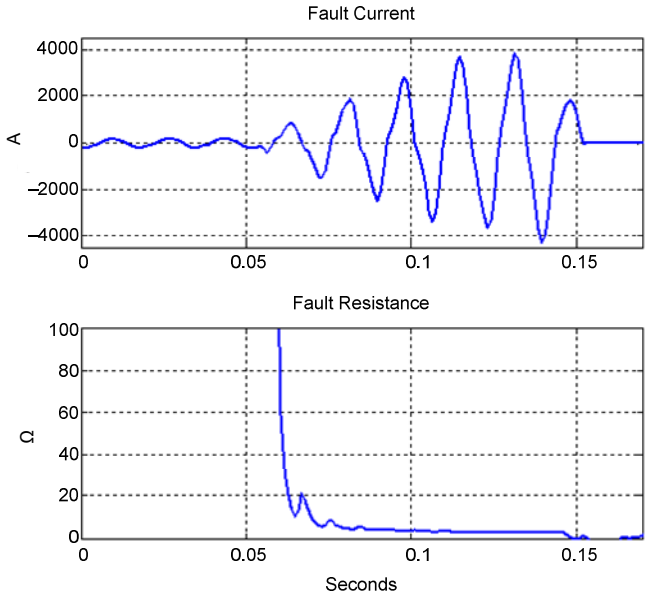

Fig. 3. Fault current and resistance for a phase-to-ground fault on a 225-kilometer, 400 kV line.

Without proper event report alignment, the rapid change of fault resistance in Fig. 3 at the start of the fault can cause additional errors when estimating fault location in transmission line applications with fast fault-clearing times. Accurate time stamping of the measurements improves event report alignment and minimizes errors caused by variable fault resistance.

IV. New Fault Location Method

Most faults on power transmission lines are unbalanced faults. The common characteristic of unbalanced faults is that there are negative-sequence currents and voltages available for the fault location calculation. This method uses an existing algorithm to distinguish between unbalanced and balanced faults [7]. Fig. 4b illustrates the negative-sequence network of the transmission line with the three line sections shown in Fig. 4a. The fault is on Section 2; *m* is the distance to the fault in per unit of the section length, as measured from Junction D.

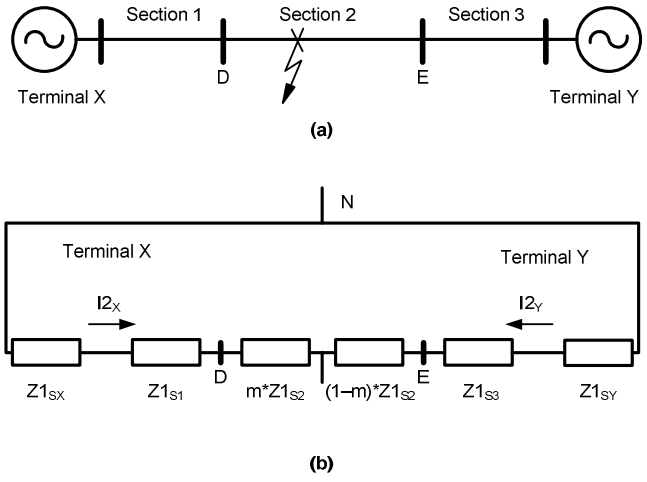

Fig. 4. (a) Transmission line with three line sections. (b) Negative-sequence network of the transmission line for a fault on Section 2.

The estimated fault location based on the negative-sequence network is not affected by zero-sequence mutual coupling and errors in zero-sequence line impedance. Accurate zero-sequence line impedances are often difficult to obtain. For underground cables in particular, the actual zero-sequence impedance depends on the bonding method of the shield and the cable configuration [8].

Another benefit of using negative-sequence quantities is that the line-charging currents have negligible impact on the accuracy of the fault location estimation because the negative-sequence voltage is significantly lower than the positive-sequence voltage along the transmission line.

The proposed method uses the profile of the estimated negative-sequence voltage magnitude along the transmission line to determine the fault location. This method identifies the faulted line section and estimates the distance to the fault in this section.

A. Identification of the Faulted Line Section

We estimate negative-sequence voltage at each junction between line sections twice, starting from each line terminal, in order to construct two negative-sequence voltage profiles. Therefore, for each line section, there are two calculated voltages for the left junction and two calculated voltages for the right junction. The intersection point of the two voltage magnitude profiles calculated from each terminal is the negative-sequence voltage magnitude at the fault location.

For a power transmission line that consists of *N* homogeneous line sections, the negative-sequence voltages at the junctions of line section *k* can be calculated using (3) through (6). The left terminal of the line is denoted as Terminal X, and the right terminal of the line is denoted as Terminal Y.

$$V2_{k\_L\_X} = V2_{meas\_X} - \sum_{i=1}^{k-1} Z1_i \bullet I2_{meas\_X} \quad (3)$$

$$V2_{k\_R\_X} = V2_{meas\_X} - \sum_{i=1}^{k} Z1_i \bullet I2_{meas\_X} \quad (4)$$

$$V2_{k\_L\_Y} = V2_{meas\_Y} - \sum_{i=k}^{N} Z1_i \bullet I2_{meas\_Y} \quad (5)$$

$$V2_{k\_R\_Y} = V2_{meas\_Y} - \sum_{i=k+1}^{N} Z1_i \bullet I2_{meas\_Y} \quad (6)$$

where:

$V2_{meas\_X}$, $I2_{meas\_X}$, $V2_{meas\_Y}$, and $I2_{meas\_Y}$ are the negative-sequence voltage and current measurements from the Terminal X and Terminal Y relays, respectively.

$Z1_i$ is the positive-sequence impedance of line section *i*, which is the same as the negative-sequence impedance.

$V2_{k\_L\_X}$ is the negative-sequence voltage at the left junction of line section *k* that is calculated from Terminal X.

$V2_{k\_R\_X}$ is the negative-sequence voltage at the right junction of line section *k* that is calculated from Terminal X.

$V2_{k\_L\_Y}$ is the negative-sequence voltage at the left junction of line section *k* that is calculated from Terminal Y.

$V2_{k\_R\_Y}$ is the negative-sequence voltage at the right junction of line section *k* that is calculated from Terminal Y.

Fig. 5 illustrates the negative-sequence voltage magnitude profiles from Terminal X and Terminal Y of the transmission line shown in Fig. 4. Because the two voltage profiles intersect at the fault location, the negative-sequence voltages at the junctions of the faulted line section meet the two criteria stated in (7) and (8).

$$\left|V2_{k\_L\_X}\right| \le \left|V2_{k\_L\_Y}\right| \quad (7)$$

$$\left|V2_{k\_R\_Y}\right| < \left|V2_{k\_R\_X}\right| \quad (8)$$

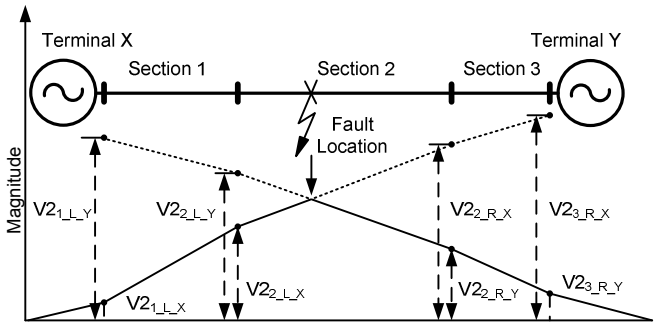

Fig. 5. Negative-sequence voltage magnitude profile along the transmission line for a fault on Section 2.

B. Estimation of the Distance to the Fault on the Faulted Line Section for Unbalanced Faults

After the algorithm identifies the faulted line section, the algorithm estimates the distance to the fault on the homogeneous line section. Fig. 6 shows the equivalent circuit of the faulted line section. The equivalent negative-sequence voltage sources, $V2_{k\_L\_X}$ and $V2_{k\_R\_Y}$, are the voltages calculated using (3) and (6) for the faulted line section.

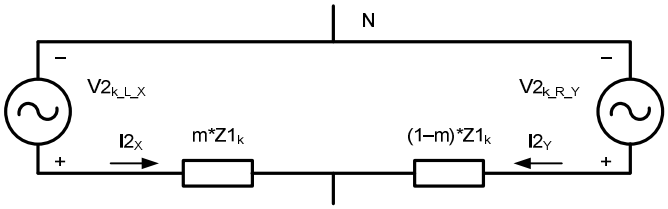

Fig. 6. Equivalent negative-sequence network for a fault on the faulted line section.

The voltage magnitudes at the fault location calculated from the two junctions should be equal to each other, according to (9). The algorithm solves (9) for the distance-to-fault value, *m*. This approach minimizes errors because of data misalignment.

$$\left|V2_{k\_L\_X} - m \bullet Z1_k \bullet I2_X\right| = \left|V2_{k\_R\_Y} - (1-m) \bullet Z1_k \bullet I2_Y\right| \quad (9)$$

C. Fault Location for Three-Phase Faults

For three-phase faults, we calculate the positive-sequence impedance to the fault, Z_{total}, from either terminal using positive-sequence voltage, V1, and current, I1, according to (10). The algorithm identifies the faulted line section, *k*, using (11). Equation (12) determines the total distance to the fault, *L*, where $Length_i$ is the length of line section *i*.

$$Z_{total} = \frac{V1}{I1} \quad (10)$$

$$\sum_{i=1}^{k-1} Zl_i \le Z_{total} < \sum_{i=1}^{k} Zl_i \quad (11)$$

$$L = \sum_{i=1}^{k-1} Length_i + \frac{Z_{total} - \sum_{i=1}^{k-1} Zl_i}{Zl_k} \bullet Length_k \quad (12)$$

V. Test Results and Field Event Case Study

This section discusses the test results and accuracy of the fault location estimation on a 26.3-mile, 230 kV transmission line. As shown in Fig. 7, this composite, nonhomogeneous line has two overhead sections and two underground cable sections. Table I lists the parameters of each line section. We used fault event reports from simulations and a field event to demonstrate the accuracy of the proposed fault location algorithm.

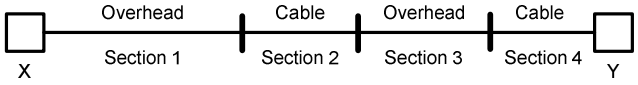

Fig. 7. Nonhomogeneous 230 kV transmission line.

Table I
Transmission Line Section Parameters

Line Section	Positive-Sequence Impedance (Ω)	Zero-Sequence Impedance (Ω)	Length (miles)
Section 1	0.9522 + j10.5536	8.4111 + j38.4107	19.0
Section 2	0.0291 + j0.4973	0.4840 + j2.6186	2.9
Section 3	0.1957 + j1.5024	1.5235 + j6.7395	4.0
Section 4	0.0026 + j0.0635	0.0661 + j0.2883	0.4

A. Test System Setup and Simulation Results

We modeled the power system that includes the transmission line shown in Fig. 7 in the Real Time Digital Simulator (RTDS®) that runs an Electromagnetic Transients Program (EMTP) simulation. Two digital line protection relays measure voltages and currents at both line terminals via the RTDS analog interface. These relays are configured to protect the transmission line using a pilot protection scheme. The relays use a demodulated IRIG-B signal as a time source.

The breaker statuses and trip signals are exchanged among the RTDS and relays via the digital I/O interface, as Fig. 8 illustrates. The system setup emulates the real-time, closed-loop controlled power system.

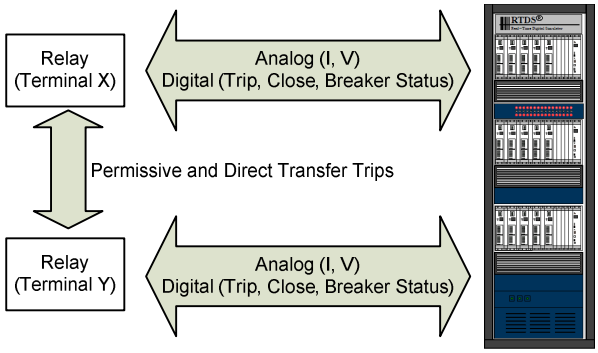

Fig. 8. Closed-loop test system includes RTDS and the two line relays.

We simulated all fault types (line-to-ground, line-to-line, line-to-line-to-ground, and three-phase) at 5.7, 13.3, and 20.16 miles from Terminal X to verify the accuracy of the proposed algorithm. The first two locations are on the first overhead section (Section 1), and the third location is on the first underground cable section (Section 2). For each fault, we collected three types of event reports from both terminals: relay-generated event reports with fixed sampling rates of 8,000 samples per second, relay-generated event reports with operating frequency-based sampling rates of 8 samples per power system cycle, and RTDS-generated event reports with fixed sampling rates of 4,000 samples per second. Fault location estimation using RTDS-generated event reports illustrates the theoretical performance of the algorithm. We use relay event reports to estimate the fault location to include the effects of relay measurement errors.

Fig. 9 shows the absolute error in fault location estimation using RTDS-generated event reports for each fault type with zero fault resistance at different locations. The largest error is 0.02 miles (106 feet), which is 0.07 percent of the total line length. Fig. 10 shows the absolute error in fault location estimation using the RTDS-generated event reports for line-to-ground faults with fault resistance varying from 0 to 100 Ω at the fault locations discussed above. The results show that the largest error is 0.04 miles (212 feet), and the fault resistance has minimal impact on the fault location estimation.

Fig. 11 shows the performance of the proposed method compared with the single-end fault location method and the existing two-end fault location method using relay-generated fixed sampling event reports. The single-end fault location method and existing two-end fault location method use only the total impedance of the composite line to estimate fault location. We obtained these event reports from simulated line-to-ground faults with fault resistance varying from 0 to 100 Ω at 20.16 miles from Terminal X.

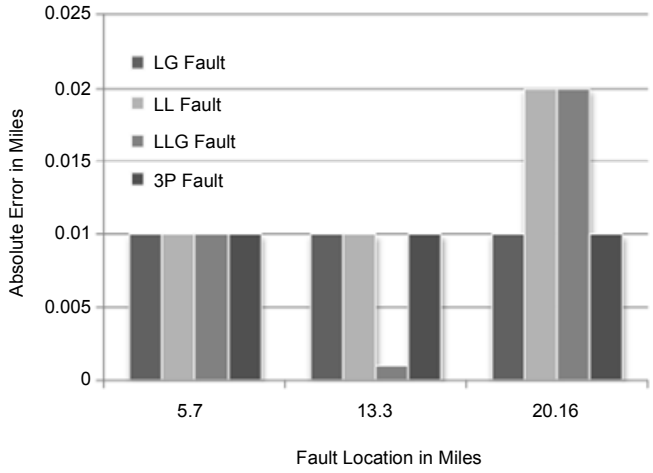

Fig. 9. Fault location errors at different locations with $R_F = 0$.

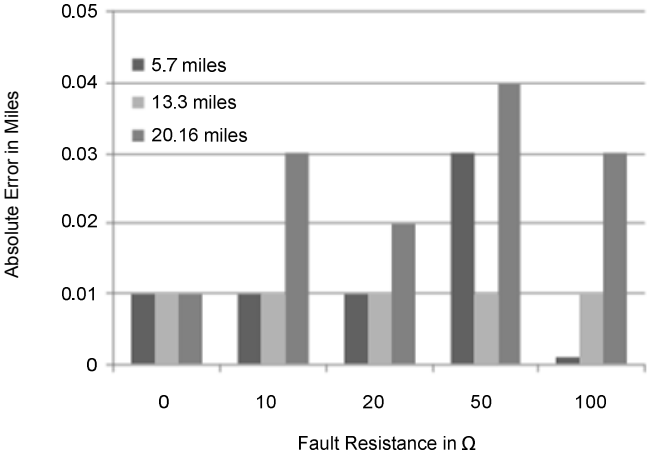

Fig. 10. Fault location errors with different fault resistances.

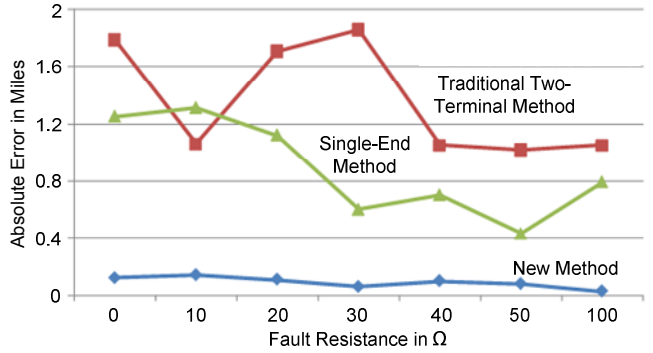

Fig. 11. Fault location error of different methods using relay event reports with fixed sampling rates for line-to-ground faults at 20.16 miles from Terminal X.

For the single-end method, relays at both terminals reported a fault location value. We selected the value with the lowest error for comparison. Fig. 11 shows that the proposed method consistently provides better fault location estimation than the traditional two-terminal and single-end methods on composite transmission lines.

Fig. 12 compares fault location errors using event reports from relays with fixed and power system operating frequency-dependent sampling rates. The results show that these two sampling methods have similar performance.

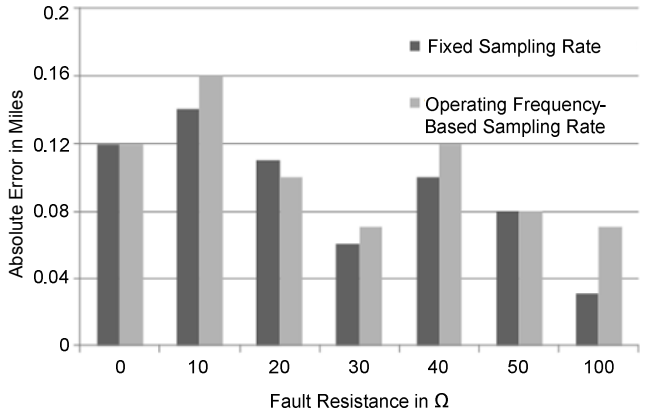

Fig. 12. Fault location errors using fixed sampling and operating frequency-based sampling event reports for line-to-ground faults at 20.16 miles.

B. Field Event Case Study

The transmission line described in Section V had an actual single-line-to-ground fault. Fig. 13 and Fig. 14 show the relay recorded current and voltage measurements for the B-phase-to-ground fault. The proposed method estimated the fault location at 18.91 miles from Terminal X. The actual fault location from line inspection was at the junction point between the first overhead line section and the first cable section, which is 19.0 miles from Terminal Y.

Table II lists the absolute errors in fault location estimation reported by the proposed method, line relays at both ends, and the traditional two-end method.

TABLE II
ABSOLUTE ERRORS OF THE ESTIMATED FAULT LOCATION IN MILES

New Method	Traditional Two-Terminal Method	Relay at Left Terminal	Relay at Right Terminal
0.09	2.18	3.91	4.25

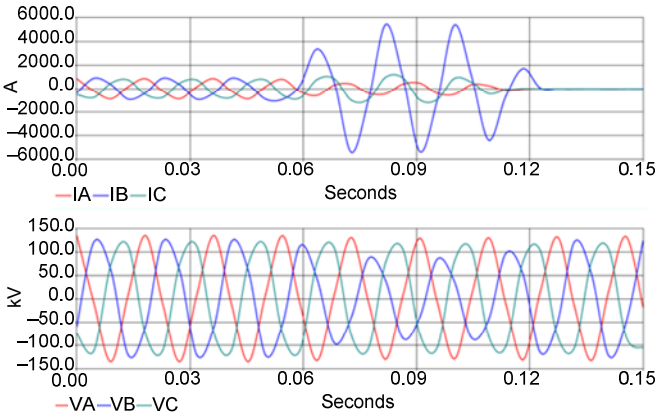

Fig. 13. Current and voltage measurements of the relay at Terminal X.

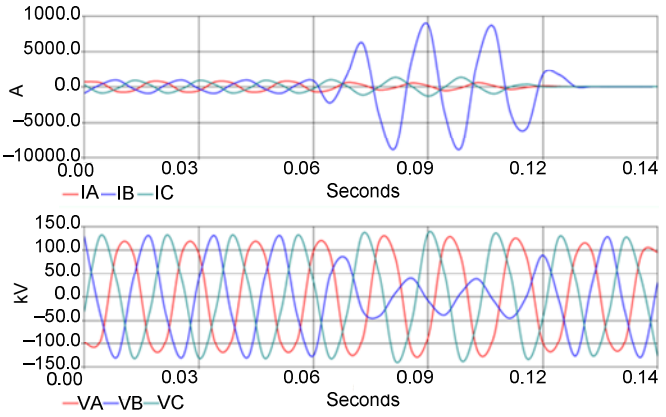

Fig. 14. Current and voltage measurements of the relay at Terminal Y.

Fig. 15 shows the negative-sequence voltage profiles calculated from both line terminals. The intersection of the two voltage profiles indicates the location of the fault. The new method provides a more accurate fault location than the existing methods (see Table II).

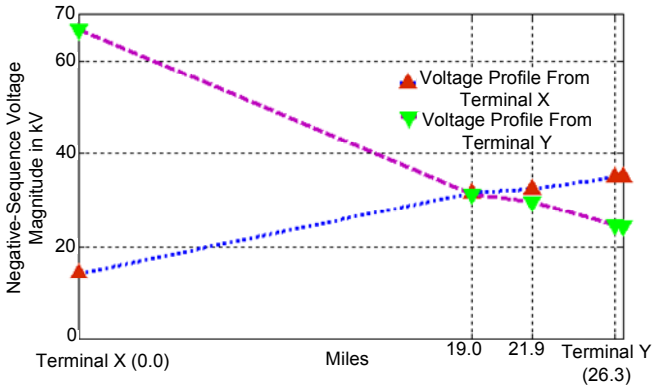

Fig. 15. Negative-sequence voltage profiles for the B-phase-to-ground fault.

VI. AUTOMATED FAULT LOCATION SYSTEM

Most of the existing multiterminal fault location methods are mainly for post-event analysis. To perform this analysis, we need to collect event reports from all line terminals, align these data, and estimate the fault location, which is time-consuming and inefficient. The automated fault location system (AFLS) that we present in this paper can monitor hundreds of transmission lines in the utility and provide fault location information in real time without human intervention. The AFLS includes protective relays connected to an IRIG-B time source and fault location software running on a computer. This software automatically retrieves event reports from the relays, calculates the fault location, and presents the results to the user. Fig. 16 shows the AFLS architecture to monitor three lines of a power system. This architecture uses Ethernet-based communication between the protective relays and the computer running the fault location software. The software accommodates serial and Ethernet communications.

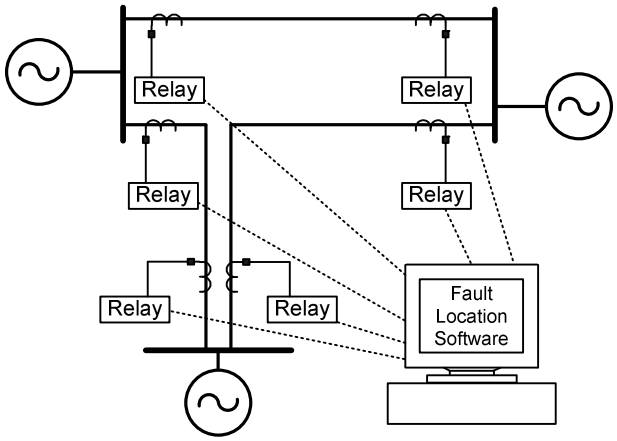

Fig. 16. AFLS monitoring three transmission lines.

A. System Configuration

The initial system configuration requires specifying the number of terminals of the monitored line, the number of sections, the section impedances, the communications parameters of the relays, and the association of the relay with the corresponding line terminal. After the system is configured, it does not require additional user intervention. The software also accommodates line terminals with dual breakers and compensates for shunt reactors based on their impedances.

B. Fault Record Retrieval and Archiving

The user can configure the fault location software to retrieve event reports from the protective relays via event-driven or polling mechanisms. When using the event-driven mechanism, the software initiates the retrieval process immediately upon receiving a message from the relay every time a new event is triggered. When using the polling mechanism, the software polls the relays for new events periodically at user-defined intervals and retrieves the new event reports. Compared to the polling mechanism, the event-driven mechanism offers lower latency and minimum communications traffic. The software stores the retrieved event reports with filenames consisting of the device name and event trigger time stamp.

C. Fault Location Calculation and Results Display

After successfully retrieving all of the event reports for a particular fault, the fault location software automatically indentifies the faulted line, estimates the fault location, and displays the results. Fig. 17 shows the display of the fault location information. This display can be available at the control center. The reported fault location information includes the line name, reference terminal, distance to the fault, fault type, and time of the fault. The software can also send the fault location information to maintenance personnel via email.

Line Name	Fault Location	From	Fault Type	Date Time
Transmission Line I	22.15	X Terminal	BG	7/29/2010 11:47 AM
Transmission Line I	7.11	X Terminal	BG	7/29/2010 11:46 AM
Transmission Line I	22.18	X Terminal	BC	7/29/2010 11:46 AM
Transmission Line I	5.77	X Terminal	ABC	7/29/2010 11:46 AM
Transmission Line I	7.15	X Terminal	BCG	7/29/2010 11:36 AM

Fig. 17. Fault location information display.

D. System Latency

The AFLS latency depends on the event retrieval time and fault location computation time. The event retrieval time depends on the communications medium between the computer and the relays. For serial communication, the event retrieval time is a function of the data transfer rate and the file size. Typically, event retrieval times are in the order of 1 to 3 minutes. For Ethernet-based communication, event retrieval times are in the order of seconds. The computer performs fault location calculations in less than 1 second. For systems with Ethernet communication, the overall system latency is less than 1 minute.

VII. AFLS Deployment

Orange and Rockland Utilities, Inc. (ORU) proposed the installation of fault-locating equipment at transmission line terminals in order to implement the two-end fault location system as part of the ORU Smart Grid Project. The majority of ORU 345/138 kV transmission lines are overhead conductors, and some of them are underground cables. These transmission lines are relatively short, approximately 9 to 10 miles; however, the lines are not easily accessible for inspection during faults due to difficult terrain. Therefore, a tool to precisely calculate the fault location is important for quick restoration of the faulted transmission line.

The algorithm presented in this paper for fault location on transmission lines using a two-ended technique, as per ORU design requirements, was tested, and the results are within 1.5 percent accuracy. Based on successful testing results, ORU allocated funding to implement this fault location technique on critical transmission lines.

ORU is planning to use relays with fixed sampling rates and accurate time stamping for fault locating. These relays can have up to six sets of three-phase current and two sets of three-phase voltage inputs. Thus, the relays can monitor multiple lines within a substation.

ORU is in the process of implementing its first double-ended fault location system. This system will include relays at each terminal of the transmission line and will communicate with a workstation located at the ORU Energy Control Center via serial communication over optical fiber. The workstation will process the fault data recorded by relays. The results, including calculated fault location, will be emailed to the system operator.

VIII. Conclusion

This paper presents an automated fault location system for transmission networks. The system uses a new multi-end fault location algorithm that is suitable for composite transmission lines. The fault location algorithm and the automated system have the following characteristics:

- The algorithm uses the negative-sequence voltage profile along the transmission line to identify the faulted section, makes a network reduction, and estimates the fault location.
- A field case validates the accuracy of the algorithm for a phase-to-ground fault on a 26.3-mile 230 kV composite line. In this case, the fault location estimation is off by 475 feet.
- After the user configures the system, the system reports fault location information in less than 1 minute when using Ethernet-based communication without human intervention.
- The system works with existing protective relays to provide an economical real-time fault location solution.
- Event reports with accurate time stamps improve multiterminal fault location accuracy, particularly for faults with varying fault resistance.

IX. Acknowledgment

The authors would like to thank Tariq Rahman of San Diego Gas and Electric for providing the line parameters and fault event reports of the field case presented in this paper.

X. References

[1] E. O. Schweitzer, III, "Evaluation and Development of Transmission Line Fault-Locating Techniques Which Use Sinusoidal Steady-State Information," proceedings of the 9th Annual Western Protective Relay Conference, Spokane, WA, October 1982.

[2] T. Takagi, Y. Yamakoshi, M. Yamaura, R. Kondow, and T. Matsushima, "Development of a New Type Fault Locator Using the One-Terminal Voltage and Current Data," *IEEE Transactions on Power Apparatus and Systems*, Vol. PAS-101, Issue 8, August 1982, pp. 2892–2898.

[3] D. A. Tziouvaras, J. Roberts, and G. Benmouyal, "New Multi-Ended Fault Location Design for Two- or Three-Terminal Lines," proceedings of the 7th International Conference on Developments in Power System Protection, Amsterdam, Netherlands, April 2001.

[4] K. Zimmerman and D. Costello, "Impedance-Based Fault Location Experience, " proceedings of the 31st Annual Western Protective Relay Conference, Spokane, WA, October 2004.

[5] D. Novosel, D. G. Hart, E. Udren, and J. Garitty, "Unsynchronized Two-Terminal Fault Location Estimation," *IEEE Transactions on Power Delivery*, Vol. 11, Issue 1, January 1996.

[6] S. Lopez, J. Gomez, R. Cimadevilla, and O. Bolado, "Synchrophasor Applications of the National Electric System Operator of Spain," proceedings of the 34th Annual Western Protective Relay Conference, Spokane, WA, October 2007.

[7] A. Guzmán, V. Mynam, and G. Zweigle, "Backup Transmission Line Protection for Ground Faults and Power Swing Detection Using Synchrophasors," proceedings of the 34th Annual Western Protective Relay Conference, Spokane, WA, October 2007.

[8] J. Vargas, A. Guzmán, and J. Robles, "Underground/Submarine Cable Protection Using a Negative-Sequence Directional Comparison Scheme," proceedings of the 26th Annual Western Protective Relay Conference, Spokane, WA, October 1999.

XI. Biographies

Yanfeng Gong received his BSEE from Wuhan University, China, in 1998, his MSEE from Michigan Technological University in 2002, and his PhD in electrical engineering from Mississippi State University in 2005. He is currently working as a research engineer at Schweitzer Engineering Laboratories, Inc., in Pullman, Washington. He is a member of IEEE.

Mangapathirao Mynam received his MSEE from the University of Idaho in 2003 and his BE in electrical and electronics engineering from Andhra University College of Engineering, India, in 2000. He joined Schweitzer Engineering Laboratories, Inc. (SEL) in 2003 as an associate protection engineer in the engineering services division. He is presently working as a lead research engineer in SEL research and development. He was selected to participate in the U.S. National Academy of Engineering (NAE) 15th Annual U.S. Frontiers of Engineering Symposium. He is a member of IEEE.

Armando Guzmán received his BSEE with honors from Guadalajara Autonomous University (UAG), Mexico. He received a diploma in fiber-optics engineering from Monterrey Institute of Technology and Advanced Studies (ITESM), Mexico, and his MSEE from the University of Idaho, USA. He served as regional supervisor of the Protection Department in the Western Transmission Region of the Federal Electricity Commission (the Mexican electrical utility company) in Guadalajara, Mexico, for 13 years. He lectured at UAG and the University of Idaho in power system protection and power system stability. Since 1993, he has been with Schweitzer Engineering Laboratories, Inc., in Pullman, Washington, where he is a research engineering manager. He holds numerous patents in power system protection and metering. He is a senior member of IEEE.

Gabriel Benmouyal, P.E., received his BASc in electrical engineering and his MASc in control engineering from Ecole Polytechnique, Université de Montréal, Canada, in 1968 and 1970. In 1969, he joined Hydro-Québec as an instrumentation and control specialist. He worked on different projects in the fields of substation control systems and dispatching centers. In 1978, he joined IREQ, where his main fields of activity were the application of microprocessors and digital techniques for substations and generating station control and protection systems. In 1997, he joined Schweitzer Engineering Laboratories, Inc., as a principal research engineer. Gabriel is an IEEE senior member and a registered professional engineer in the Province of Québec and has served on the Power System Relaying Committee since May 1989. He holds over six patents and is the author or coauthor of several papers in the fields of signal processing and power network protection and control.

Boris Shulim is a principal transmission relay protection and system planning engineer for Orange and Rockland Utilities, Inc. (ORU) in Spring Valley, New York. Boris is a graduate of Polytechnic Institute of Kishinev, Russia. Since 1985, he has been employed by ORU. His responsibilities have included the application and design of protective relay systems, coordination and settings studies, and the analysis of relay performance during system disturbances. Boris has extensive experience with field troubleshooting and relay and control testing. He is a professional engineer in the state of New York.